Article

TRANSPARENT
PROCESS

THE
EMBO
JOURNAL

Tubulin glycylases are required for primary cilia, control of cell proliferation and tumor development in colon

Cecilia Rocha[1,2,3,4,5,6], Laura Papon[5,6], Wulfran Cacheux[7], Patricia Marques Sousa[1,2,3,4], Valeria Lascano[8], Olivia Tort[1,2,3,4,9], Tiziana Giordano[1,2,3,4], Sophie Vacher[7], Benedicte Lemmers[5,6], Pascale Mariani[7], Didier Meseure[7], Jan Paul Medema[8], Ivan Bièche[7], Michael Hahne[5,6,8,**,†] & Carsten Janke[1,2,3,4,*,†]

Abstract

TTLL3 and TTLL8 are tubulin glycine ligases catalyzing posttranslational glycylation of microtubules. We show here for the first time that these enzymes are required for robust formation of primary cilia. We further discover the existence of primary cilia in colon and demonstrate that TTLL3 is the only glycylase in this organ. As a consequence, colon epithelium shows a reduced number of primary cilia accompanied by an increased rate of cell division in TTLL3-knockout mice. Strikingly, higher proliferation is compensated by faster tissue turnover in normal colon. In a mouse model for tumorigenesis, lack of TTLL3 strongly promotes tumor development. We further demonstrate that decreased levels of TTLL3 expression are linked to the development of human colorectal carcinomas. Thus, we have uncovered a novel role for tubulin glycylation in primary cilia maintenance, which controls cell proliferation of colon epithelial cells and plays an essential role in colon cancer development.

Introduction

Tubulin posttranslational modifications play key roles in the regulation of the microtubule (MT) cytoskeleton. Most of the known modifications occur on the C-terminal tail domains of tubulin molecules and are therefore exposed to the outer surface of MTs where essential interactions with diverse MT-associated proteins take place (reviewed in: Janke & Bulinski, 2011). Particularly complex modification patterns are generated by posttranslational addition of glutamate or glycine side chains to the C-terminal tubulin tails (Eddé et al, 1990; Redeker et al, 1994). In mammals, glutamylation has been found in a variety of cells and tissues; however, particularly high levels have been found on neuronal MTs (Audebert et al, 1994), centrioles (Bobinnec et al, 1998) and on the axonemes of cilia and flagella (Gagnon et al, 1996; Million et al, 1999). Glycylation, in contrast, has so far been found exclusively in axonemes of motile cilia and flagella in a wide variety of organisms (Bré et al, 1996). Only in some organisms, such as the unicellular ciliate *Paramecium*, cytoplasmic MTs are also glycylated (Bré et al, 1998).

Both MT glutamylation and glycylation have been shown to play important roles in the function of motile cilia and flagella in several organisms. While glycylation has been linked to the stability and maintenance of these organelles, glutamylation has been found to play a role in the coordination of ciliary beating (Xia et al, 2000; Pathak et al, 2007, 2011; Rogowski et al, 2009; Wloga et al, 2009; Kubo et al, 2010; Suryavanshi et al, 2010; Bosch Grau et al, 2013). In contrast, less is known about the role of these two modifications in primary cilia. So far, only a link between aberrant glutamylation

1 Institut Curie, Orsay, France
2 PSL Research University, Paris, France
3 CNRS UMR3306, Orsay, France
4 INSERM U1005, Orsay, France
5 IGMM, CNRS UMR5535, Montpellier, France
6 Université Montpellier Sud de France, Montpellier, France
7 Institut Curie Hospital, Paris, France
8 Academic Medical Center, Amsterdam, The Netherlands
9 Institut de Biotecnologia i de Biomedicina, Department of Biochemistry and Molecular Biology, Universitat Autònoma de Barcelona, Bellaterra (Barcelona), Spain
   *Corresponding author. Tel: +33 1 69863127; Fax: +33 1 69863017; E-mail: carsten.janke@curie.fr
   **Corresponding author. Tel: +33 4 67613639; Fax: +33 4 34359634; E-mail: hahne@igmm.cnrs.fr
   †These authors contributed equally to the work

and defects of primary cilia has been reported (Lee *et al*, 2012, 2013).

In mammals, tubulin glutamylation can be catalyzed by nine glutamate ligases, also referred to as glutamylases or polyglutamylases (van Dijk *et al*, 2007), while only two enzymes, TTLL3 and TTLL8, are able to initiate glycylation on MTs (Rogowski *et al*, 2009). These two glycylases appear to be partially complementary in the generation of MT glycylation, as only absence of both enzymes led to the loss of motile cilia from ependymal cells in the brain ventricles (Bosch Grau *et al*, 2013). This finding further suggested that glycylation is an essential stabilizer of motile cilia in mammals, but let open the question of the role of this modification in primary cilia.

In the present work, we address the impact of MT glycylation on the integrity of primary cilia and study the role of glycylases in tissue homeostasis and colorectal cancer development. We found that TTLL3 is the only glycylase expressed in colon. Absence of *TTLL3*, synonymous for absence of glycylation in colon, leads to reduction of the number of primary cilia in colon accompanied by a strong increase in cell proliferation in the colon epithelium. In mouse embryonic fibroblasts, which express two glycylases (TTLL3, TTLL8), primary cilia are lost only upon depletion of both genes. This demonstrates that glycylation is important for primary cilia maintenance, which controls cell cycle and tissue homeostasis at least in colon epithelium. Finally, we established the relevance of TTLL3 for colon cancer development by demonstrating the impact of this gene in a mouse model for colitis-associated colon cancer, which is coherent with a significant downregulation of *TTLL3* expression in patients with colorectal cancer.

Results

Glycylating enzymes are important for maintenance of primary cilia

Glycylation has so far only been observed in motile cilia; however, nothing is known about the presence and the role of this modification in primary cilia. To investigate the role of glycylating enzymes for primary cilia, we used mouse embryonic fibroblasts (MEFs) that express both glycylating enzymes, *TTLL3* and *TTLL8* (Fig 1A). MEFs were grown *in vitro* and serum-deprived to assemble primary cilia. Cilia and their basal bodies were visualized with antibodies for acetylated α-tubulin and γ-tubulin, respectively (Fig 1B). Quantification of cilia numbers revealed that most of the cultured MEFs grow primary cilia in control and *ttll3⁻ᐟ⁻* MEFs (Fig 1C). This indicates that loss of the glycylase TTLL3 does not affect primary cilia in MEFs, which is similar to our observations in motile cilia of ependymal cells (Bosch Grau *et al*, 2013).

Glycylation has so far not been reported in primary cilia. Using the monoglycylation-specific antibody TAP952 (Bré *et al*, 1996), we detected glycylation in primary cilia of both control and *ttll3⁻ᐟ⁻* MEFs, confirming that glycylation in these cilia can be present, even in absence of TTLL3, indicating that the modification is carried out by TTLL8 alone (Fig 1D). The relatively weak labeling of primary cilia grown on MEFs could be due either to relatively low glycylation levels in these very short primary cilia, or to the presence of alternative modification sites on tubulin that are not detected by TAP952. Thus, TAP952 might not be an optimal marker for glycylation

of primary cilia, but is sufficient to prove the presence of this modification in these organelles.

We next studied the impact of the loss of both *TTLL3* and *TTLL8* on primary cilia in MEFs. For this, control and *ttll3⁻ᐟ⁻* MEFs were transfected with vectors expressing shRNA for TTLL8 and CFP. Ciliogenesis was subsequently induced by serum starvation. Transfected cells were identified by CFP fluorescence, and primary cilia were labeled with anti-acetylated tubulin and anti-γ-tubulin antibodies (Fig 1E). The percentage of CFP-positive cells that carry a primary cilium was determined (Fig 1F). Expression of scrambled shRNA had no effect on ciliogenesis in control and *ttll3⁻ᐟ⁻* MEFs, while depletion of *TTLL8* with two different shRNA constructs reduced the number of ciliated cells by about 50% specifically in the *ttll3⁻ᐟ⁻* MEFs. This shows that the absence of both glycylating enzymes, TTLL3 and TTLL8, either induces ciliary loss or disturbs the assembly of primary cilia (Fig 1F). Thus, primary cilia are, similar to their motile counterparts, dependent on glycylation. This was unexpected, as glycylation had never been detected in primary cilia before.

TTLL3 is the only glycylase expressed in the murine colon

To investigate whether both glycylases are present throughout the mammalian organism, we analyzed the expression levels of *TTLL3* and *TTLL8* in a set of normal mouse tissues using reverse-transcriptase PCR (qRT-PCR). While the relative expression levels of the two glycylases varied between tissues, both enzymes were detected in most of the tissues analyzed, with the exception of colon, where only *TTLL3* was found (Fig 2A).

To exclude the expression of trace amounts of *TTLL8* in colon, we amplified *TTLL3* and *TTLL8* with RT-PCR using a very high number of PCR cycles. As controls, we used two tissues that assemble motile, highly glycylated cilia, that is, trachea and testis. Both, *TTLL3* and *TTLL8* are expressed in trachea and testes of wild-type mice, while no expression of *TTLL8* was detected in colon, even after 40 PCR cycles (Fig 2B). The results of the PCR also corroborated the absence of *TTLL3* in all tested tissues of *ttll3⁻ᐟ⁻* mice.

To localize the expression of *TTLL3* in colon tissue, we used *ttll3⁻ᐟ⁻* mice that carry a β-galactosidase insertion within the region of the *TTLL3* gene. *TTLL3* expression, visualized by staining with 5-bromo-4-chloro-3-indolyl-β-D-galactopyranoside (X-gal), was detected in the epithelial cells from the bottom up to the top of the crypts. This indicates that *TTLL3* is expressed throughout the colon crypts (Fig 2C). The β-galactosidase activity and thus *TTLL3* expression were comparable between colon and testis confirming the qRT-PCR analysis (Fig 2A).

We therefore conclude that the only enzyme available for catalyzing glycylation in colon is TTLL3. Consequently, downregulation, loss or enzymatic inactivation of *TTLL3* are expected to result in the absence or at least in a decrease of glycylating activity in colon cells and should directly engender a loss of primary cilia.

Absence of TTLL3 leads to reduced numbers of primary cilia in colon epithelium

As primary cilia have so far not been described in colon tissue, we investigated ciliogenesis on cultured colon epithelial cells (CECs). Confluent cultured CECs from control and *ttll3⁻ᐟ⁻* mice were grown for 2 days under serum starvation and subsequently immunolabeled
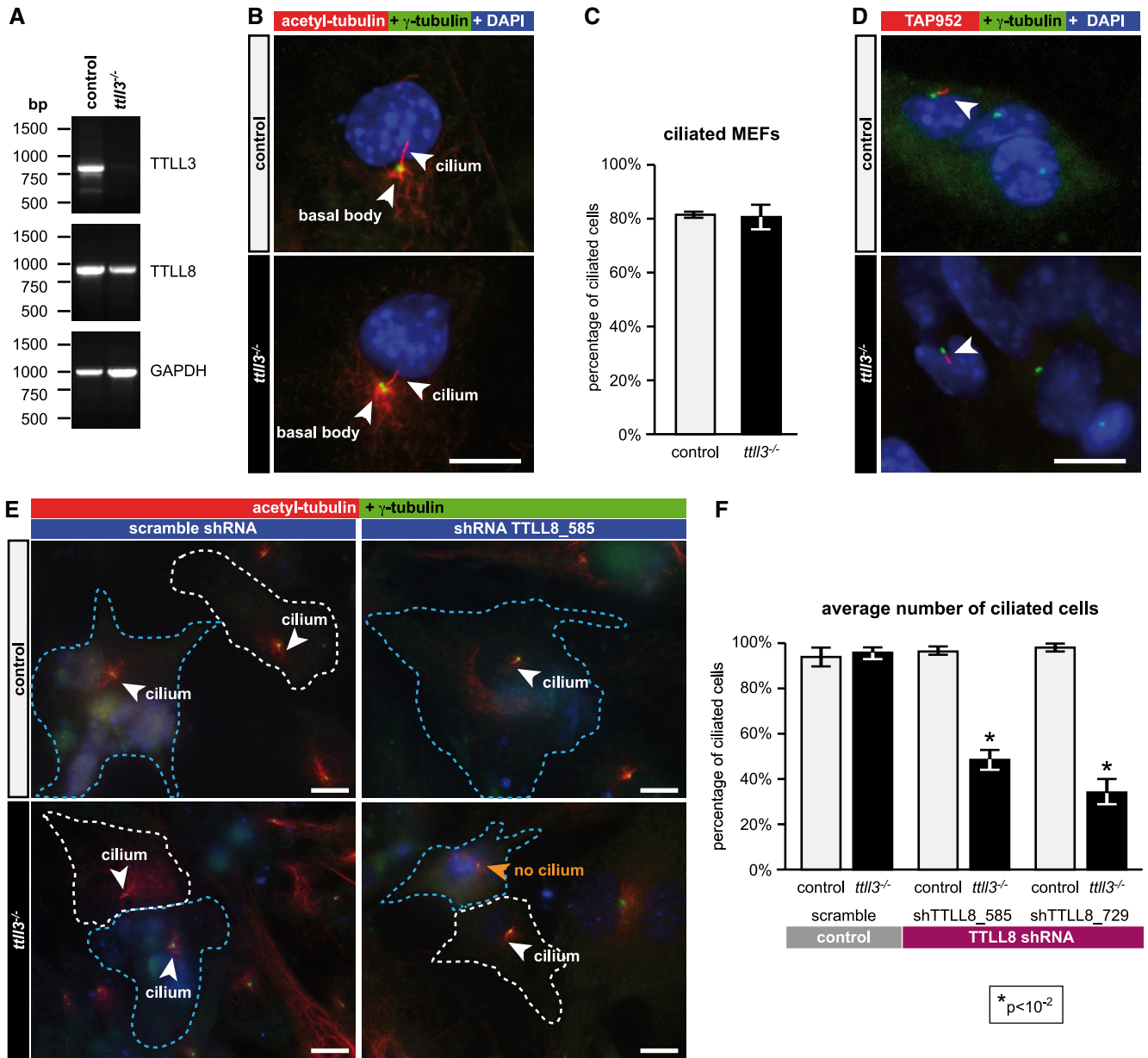
Figure 1. Glycylating enzymes and primary cilia formation in MEFs.

A   The expression of *TTLL3* and *TTLL8* was analyzed by RT-PCR in samples from control and *ttll3*$^{-/-}$ MEFs.

B   Wild-type and *ttll3*$^{-/-}$ MEFs were serum-starved for 2 days and labeled with anti-acetylated tubulin (red) and anti-γ-tubulin (green) antibodies, and nuclei were stained with DAPI (blue).

C   Percentage of ciliated cells (analyzed from B). Mean values ± SEM are represented (control n = 4 mice; *ttll3*$^{-/-}$ n = 4 mice; 50 cells counted per mouse).

D   MEFs as in (B) were stained with TAP952 (red) for monoglycylation. Arrowheads indicate TAP952-positive primary cilia.

E   MEFs were transfected with vectors coding for scramble and *TTLL8* shRNA and CFP and starved for 24 h. Primary cilia were visualized with anti-acetylated tubulin (red) and anti-γ-tubulin (green) antibodies. Transfected cells were identified by CFP (blue). Blue lines indicate transfected, and white lines non-transfected cells. Cilia are indicated by white arrowheads, and absence of cilia (identified by solitary basal bodies) by orange arrowheads.

F   Percentage of transfected, ciliated MEFs after scramble shRNA (control, n = 210 cells; *ttll3*$^{-/-}$ n = 170 cells), *TTLL8* shRNA_585 (control n = 130 cells; *ttll3*$^{-/-}$ n = 130 cells) and *TTLL8* shRNA_729 (control n = 175 cells; *ttll3*$^{-/-}$ n = 210 cells). Data represent mean values of four independent experiments ± SEM; *$P < 10^{-2}$ by two-tailed unpaired *t*-tests and Mann–Whitney post-test.

Data information: Scale bars in (B), (D) and (E) are 10 μm.

with antibodies for E-cadherin (to identify epithelial cells) and for detyrosinated α-tubulin (a specific marker of cilia and centrioles). Anti-detyrosinated tubulin staining clearly visualized short primary cilia on cultured CECs and identified the basal bodies (or centrosomes) of those cells that did not grow cilia (Fig 3A). Counting the number of ciliated CECs in densely grown regions of the cell
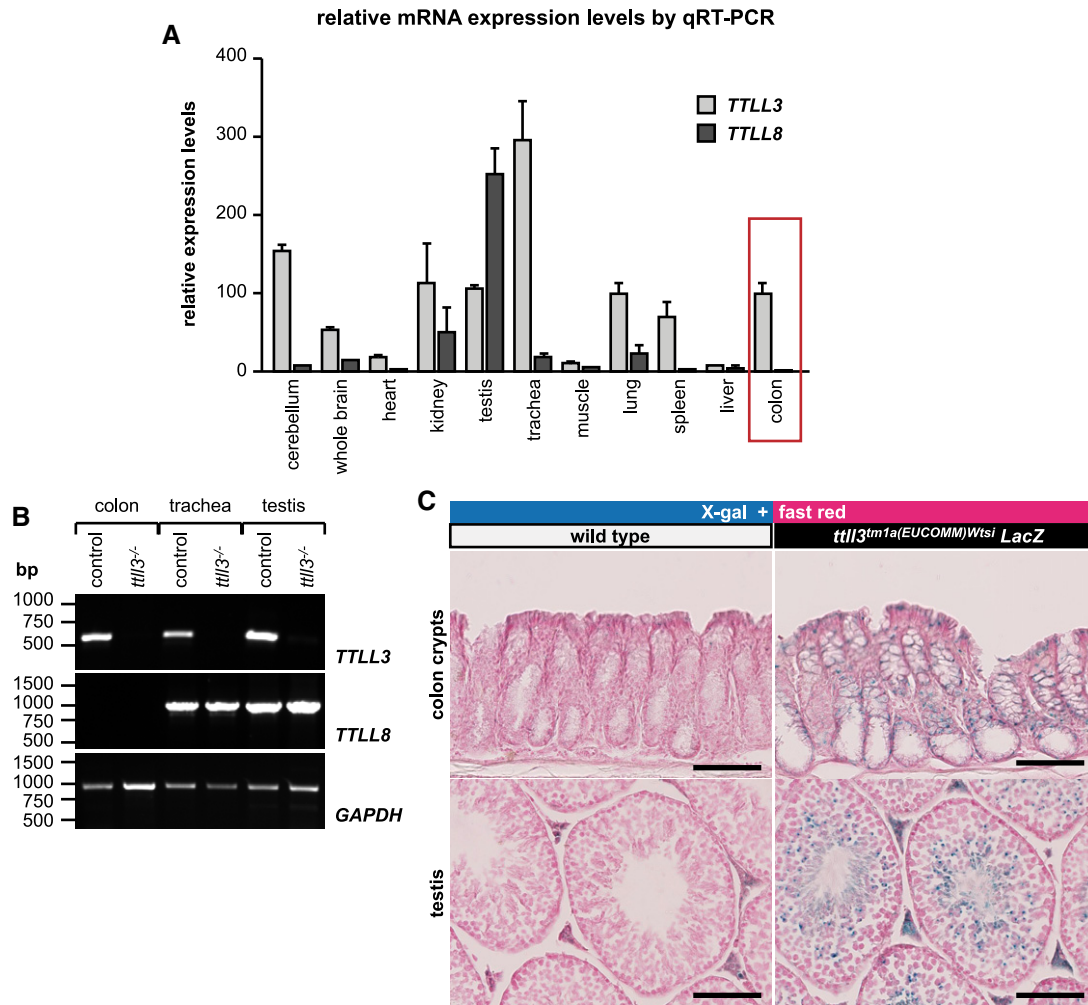
Figure 2. TTLL3 is the only glycylase expressed in colon.

A Expression levels of *TTLL3* and *TTLL8* analyzed in tissues of 4-month-old wild-type mice. Five independent mRNA samples were analyzed by qRT-PCR, and mean values standardized to expression of *Tbp* are shown. Error bars represent SEM. Red box: note that no *TTLL8* expression is detected in colon tissue.

B *TTLL3* and *TTLL8* expression analysis by RT-PCR in 4-month-old control and *ttll3⁻/⁻* mice. TTLL3 expression is completely abolished in all tissues tested in *ttll3⁻/⁻* mice, while TTLL8 expression levels are unchanged. No *TTLL8* expression was detected in colon.

C Expression of *TTLL3* detected by *TTLL3*-promoter–β-galactosidase (blue) on colon and testis tissue sections from 4-month-old mice. Scale bars are 100 μm. Tissues are counterstained with Nuclear Fast Red.

cultures revealed a more than threefold decrease in the number of ciliated CECs from *ttll3⁻/⁻* mice as compared to controls (Fig 3B).

To confirm the presence of primary cilia in colon epithelium *in vivo*, we investigated histological sections of mouse colon by immuno-fluorescence using different ciliary markers. We found, however, that many typical cilia markers such as antibodies for detyrosinated or acetylated tubulin failed to detect specifically primary cilia in colon tissue, which is in agreement with a previous report (Saqui-Salces *et al*, 2012). Only an antibody for Arl13b, a specific marker of primary cilia (Caspary *et al*, 2007), allowed us to detected primary cilia in the epithelial layers of the crypts (Fig 3C). Yet, only a small amount of epithelial cells were identified as being ciliated, most likely due to difficulties with antibody accessibility in the tissue. Despite these technical limitations, quantitative analysis of the number of clearly identifiable Arl13b-positive cilia demonstrated a reduction of the average number of cilia per crypt in *ttll3⁻/⁻* colons (Fig 3D). While the

numbers of cilia per crypt varied between crypts within each colon analyzed, the mean values were strikingly similar between different animals, thus confirming a reproducible and significant decrease in the number of cilia in colon crypts of *ttll3⁻/⁻* mice (Fig 3E).

Thus, colonic epithelial cells are able to form primary cilia, and lose cilia upon depletion of the unique glycylase TTLL3 in culture as well as *in vivo*. Together with the observations in MEFs (Fig 1) and ependymal cells (Bosch Grau *et al*, 2013), our results support a model in which the majority of cilia, primary as well as motile, depend on posttranslational glycylation. However, in the case of primary cilia, absence of glycylation leads only to a partial loss of cilia.

Loss of TTLL3 results in increased cell proliferation in colon

Primary cilia have been implicated in the control of cell division, tissue homeostasis and signaling (Lin *et al*, 2003; Croyle *et al*,
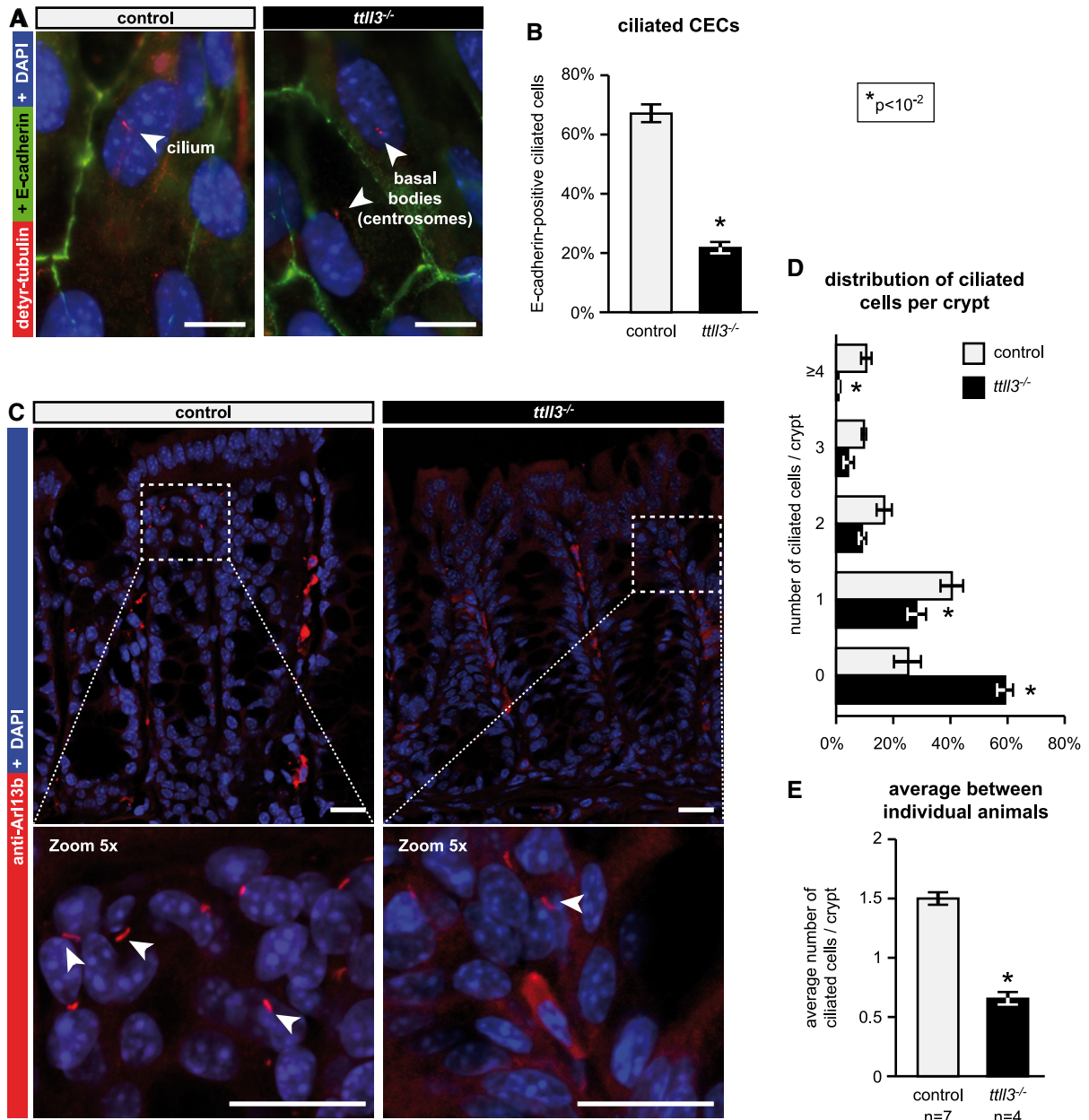
Figure 3. Primary cilia in colon epithelium.

A   Colon epithelial cells (CECs) isolated from control ($n = 7$) and $ttll3^{-/-}$ ($n = 6$) mice at postnatal day 4 were cultured for 72–96 h and then serum-starved for 48 h. E-cadherin (green) labeling revealed adherens junctions of epithelial cells. Primary cilia and centrioles (basal body or centrosome) were visualized with the anti-detyrosinated tubulin antibody (red). Nuclei were stained with DAPI. Arrowheads indicate a representative primary cilium (control) and a basal body (or centrosome) of a non-ciliated cell ($ttll3^{-/-}$). Scale bars are 10 μm.

B   Quantification of the percentage of ciliated cells in clusters of E-cadherin-positive cells in CECs from control ($n = 859$) and $ttll3^{-/-}$ ($n = 1,183$) mice. Data are mean values ± SEM; *$P < 10^{-2}$ by two-tailed unpaired t-tests and Mann–Whitney post-test.

C   Confocal images (maximum projection) of cryo-sections from colon stained with the antibody Arl13b (red) and DAPI (blue). Arl13b specifically labels primary cilia (arrowheads). Cytoplasmic staining of stromal cells is non-specific, as Arl13b is a membrane protein (Cevik et al, 2010). The selected image shows a particularly high density of detectable primary cilia. Scale bars are 20 μm.

D   Quantification of the number of clearly detectable Arl13b-positive ciliated cells per crypt. The relative numbers of crypts with 0, 1, 2, 3, 4 and more ciliated cells are represented as mean values ± SEM between individual mice (control $n = 7$; $ttll3^{-/-}$ $n = 4$). Total number of analyzed crypts: control = 259, $ttll3^{-/-}$ = 198.

E   Average number of visualized ciliated cells per crypt. Mean values ± SEM are shown. *$P < 10^{-2}$ by two-tailed unpaired t-test and Mann–Whitney post-test.

2011; Saqui-Salces et al, 2012; Wilson et al, 2012). To explore the impact of primary cilia loss in the absence of *TTLL3*, we assessed the proliferative activity and turnover of colon epithelia cells by bromodeoxyuridine (BrdU) incorporation. BrdU was intraperitoneally injected in control and $ttll3^{-/-}$ mice, and colons were dissected 2 h or 5 days after the injection. The number and

position of BrdU-positive cells in colon crypts were assessed with anti-BrdU antibodies (Fig 4A). Two hours after injection, $ttll3^{-/-}$ colons displayed nearly four times increased number of BrdU-positive nuclei per crypt. Moreover, about 25% of these dividing cells were localized in the central region of the crypts, where virtually no proliferating cells were detected in wild-type colons (Fig 4B). Thus, the absence of TTLL3 deregulates cell division in colon epithelium.

To follow-up the fate of the faster-dividing cells, we analyzed colon tissue 5 days after BrdU injection. At this time point, the total number of BrdU-positive cells was lower in $ttll3^{-/-}$ as compared to control mice, and most of the BrdU-labeled cells in $ttll3^{-/-}$ mice were detected in the upper crypt compartment. In contrast, BrdU-positive cells were still present in the central compartment of the crypts in control animals. Thus, it appears that $ttll3^{-/-}$ mice display a higher proliferation rate that is coupled to a faster turnover of epithelial cells in the crypts. Most likely, the high dynamics of the colon tissue balances the increased proliferation of colonic epithelial cells by efficient shedding and thus maintains a normal architecture of the colon. This is underlined by the histochemical analysis of colon tissue, which revealed no obvious changes in differentiation of colon epithelial cells such as goblet cells (Supplementary Fig S1).

To confirm these observations on the cellular level, we isolated CECs from control and $ttll3^{-/-}$ mice and cultivated them for 3 days *in vitro*. DNA was stained with 7-aminoactinomycin D (7-AAD), and the DNA content per cell was determined by flow cytometry (Fig 4C). In wild-type CECs, about 20% of the cells had a DNA content of > 2n, indicative of cells that are in S or in G2 phase/metaphase of the cell cycle (S + M). In contrast, about 45% of CECs from $ttll3^{-/-}$ mice were found to contain > 2n DNA (Fig 4D). This demonstrates that cultured CECs have a significantly higher mitotic activity in the absence of *TTLL3*. As a consequence of this higher proliferation activity *in vitro*, CECs from $ttll3^{-/-}$ mice divided more rapidly, as the significantly increased cell number after 48 h *in vitro* revealed (Fig 4E).

We next compared the nuclear expression of cyclin D1, a proliferation marker (Tetsu & McCormick, 1999), between colon epithelial cells of control and $ttll3^{-/-}$ mice. The distribution of cyclin D1 (Fig 4F and G) mirrors the distribution of BrdU-positive cells 2 h after BrdU injection (Fig 4A and B), with an overall increase and a redistribution of cyclin D1-positive cells into the middle and upper part of the crypts of $ttll3^{-/-}$ colons. These findings confirm that absence of TTLL3 leads to increased cell proliferation and accelerated tissue turnover in colon epithelium.

Loss of TTLL3 results in the amplification of tumor development in mice

Despite the strongly increased proliferation rates, $ttll3^{-/-}$ mice have no gross abnormalities in colon tissue of young mice (2–3 months old). To assess the impact of TTLL3-deficiency on colon homeostasis in more detail, we examined colons of ten $ttll3^{-/-}$ mice older than 16 months. Histological analysis did not show any visible abnormality in the colon of $ttll3^{-/-}$ mice (Supplementary Fig S2). This indicates that colon tissue has a high compensatory potential for changes in proliferation rates. However, we speculated that the increased proliferation rate in TTLL3-deficient colon could promote cancer development.

To test this possibility, we used a well-established mouse model of colitis-associated carcinogenesis (Tanaka *et al*, 2003; Suzuki *et al*, 2004). In this model, initial mutagenesis is induced by the intraperitoneal injection of azoxymethane (AOM), and subsequent inflammation in the colon by periodic administration of dextrane sodium sulfate (DSS) in the drinking water (Fig 5A). At the end of the protocol, mice were dissected and colorectal tumors were classified according to tumor stage and status of the Wnt signaling pathway, a key pathway in CRC. We further visualized proliferative activity of colon cells by staining of the proliferation marker Ki-67 (Supplementary Fig S3; Schlemper *et al*, 2000; Lascano *et al*, 2012).

The colitis-associated carcinogenesis protocol (Fig 5A) was applied to a total of 26 control and 21 $ttll3^{-/-}$ mice in five independent experiments. $Ttll3^{-/-}$ mice showed an increase in tumor incidence represented by an increased total number of lesions (Fig 5B and C), as well as a significant increase of tumor size represented by the total tumor area (Fig 5B and D). Tumors in controls and $ttll3^{-/-}$ mice displayed all standard characteristics, such as the loss of goblet cell differentiation, increased expression of the proliferation marker Ki-67 (Scholzen & Gerdes, 2000) and nuclear accumulation of β-catenin (Supplementary Fig S3). Finally, we characterized the

---

**Figure 4.** Loss of *TTLL3* results in increased proliferation of colon epithelium.

A   Cell proliferation in colon crypts was analyzed by incorporation of BrdU. Representative pictures of BrdU immunohistochemistry (brown) 2 h and 5 days after intraperitoneal injection of BrdU. Paraffin-embedded colon sections from control and $ttll3^{-/-}$ mice were stained with anti-BrdU antibody and hematoxylin. Scale bar is 100 μm.

B   Quantification of BrdU-positive cells in three compartments of the crypts (see scheme) 2 h and 5 days post-injection. At least 30 crypts per mouse were counted in three (2 h) and four (5 days) independent experiments (number of mice: 2 h control n = 3; 2 h $ttll3^{-/-}$ n = 3; 5 days control n = 4; 5 days $ttll3^{-/-}$ n = 4).

C   Colon epithelial cells (CECs) from 4-month-old control and $ttll3^{-/-}$ mice were cultured for 48 h, and DNA labeled with 7-AAD was quantified by flow cytometry. Two representative DNA-content profiles are shown for wild-type and $ttll3^{-/-}$ CECs. Cells in G1 phase as well as dividing cells (S phase and mitosis; S + M) were quantified as indicated.

D   Average number of cells in division (S + M) from quantifications as in (C). Bars represent SEM between different experiments (control n = 9; $ttll3^{-/-}$ n = 6).

E   Relative increase in cell number (CECs) after 48 h in culture.

F   Representative pictures of cyclin D1 staining (brown). Paraffin-embedded colon sections from control and $ttll3^{-/-}$ mice were stained with anti-cyclin D1 antibody and hematoxylin. Scale bar is 100 μm.

G   Quantification of cyclin D1-positive cells in three compartments of the crypts (see scheme). At least 40 crypts per mouse were counted (control n = 8; $ttll3^{-/-}$ n = 8).

Data information: Mean values with bars representing SD (B, G) or SEM (C, D) are shown. Significance values were determined by two-tailed unpaired *t*-tests and Mann–Whitney post test (*$P < 10^{-2}$, **$P < 10^{-3}$).

histopathological grading of AOM/DSS-induced tumors (Schlemper *et al*, 2000).

The quantification of the severity of the detected lesions (Supplementary Fig S4) in a subset of 12 animals per group revealed a similar distribution of low-grade dysplasia, high-grade dysplasia

and intramucosal carcinoma in control and *ttll3*$^{-/-}$ mice (Fig 5E). This suggests that absence of TTLL3 supports the transformation of the colonic epithelium into neoplastic lesions resulting in an increase in number and size of tumorous lesions, but not in a progression to more severe lesions at the time point analyzed.
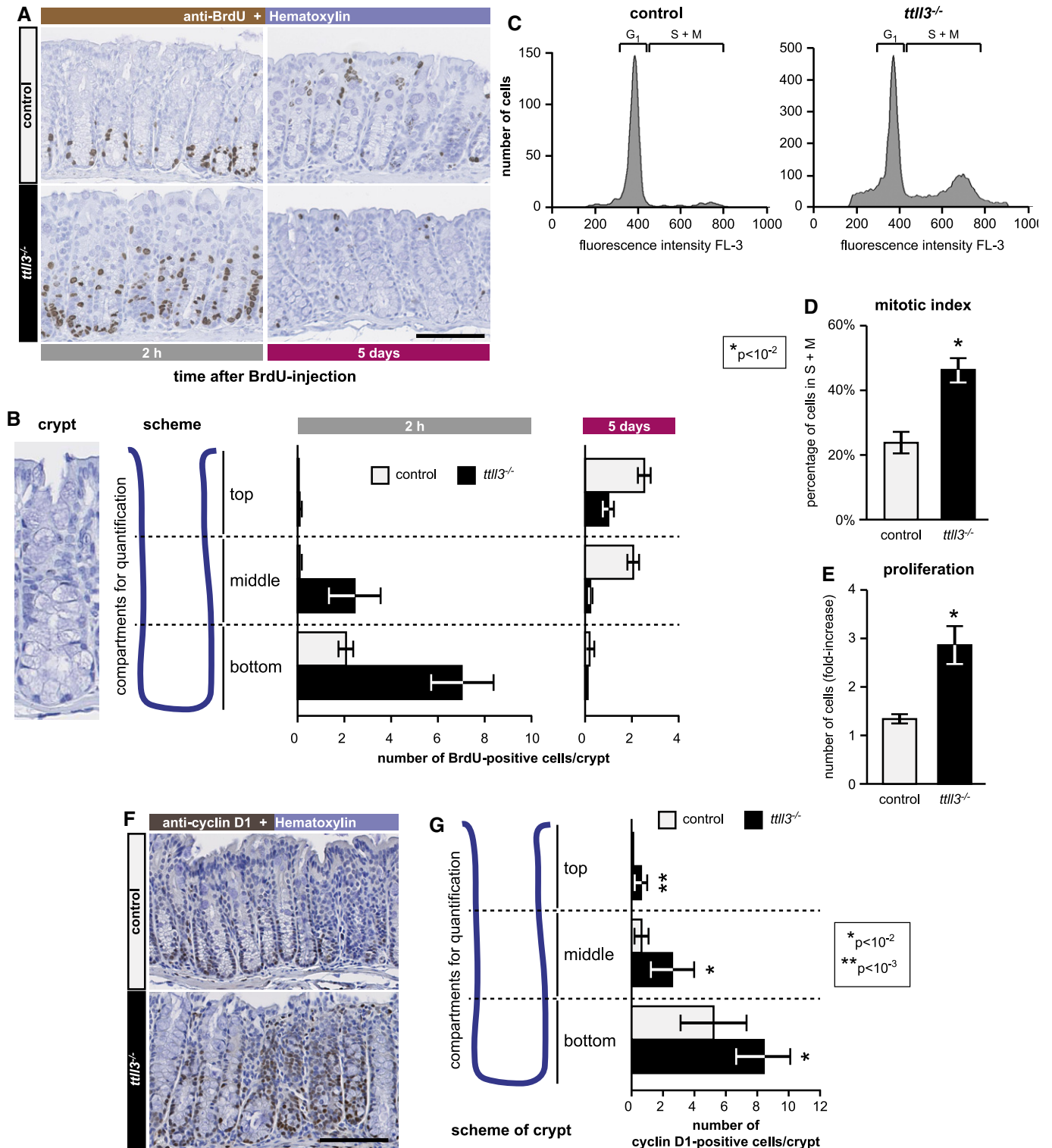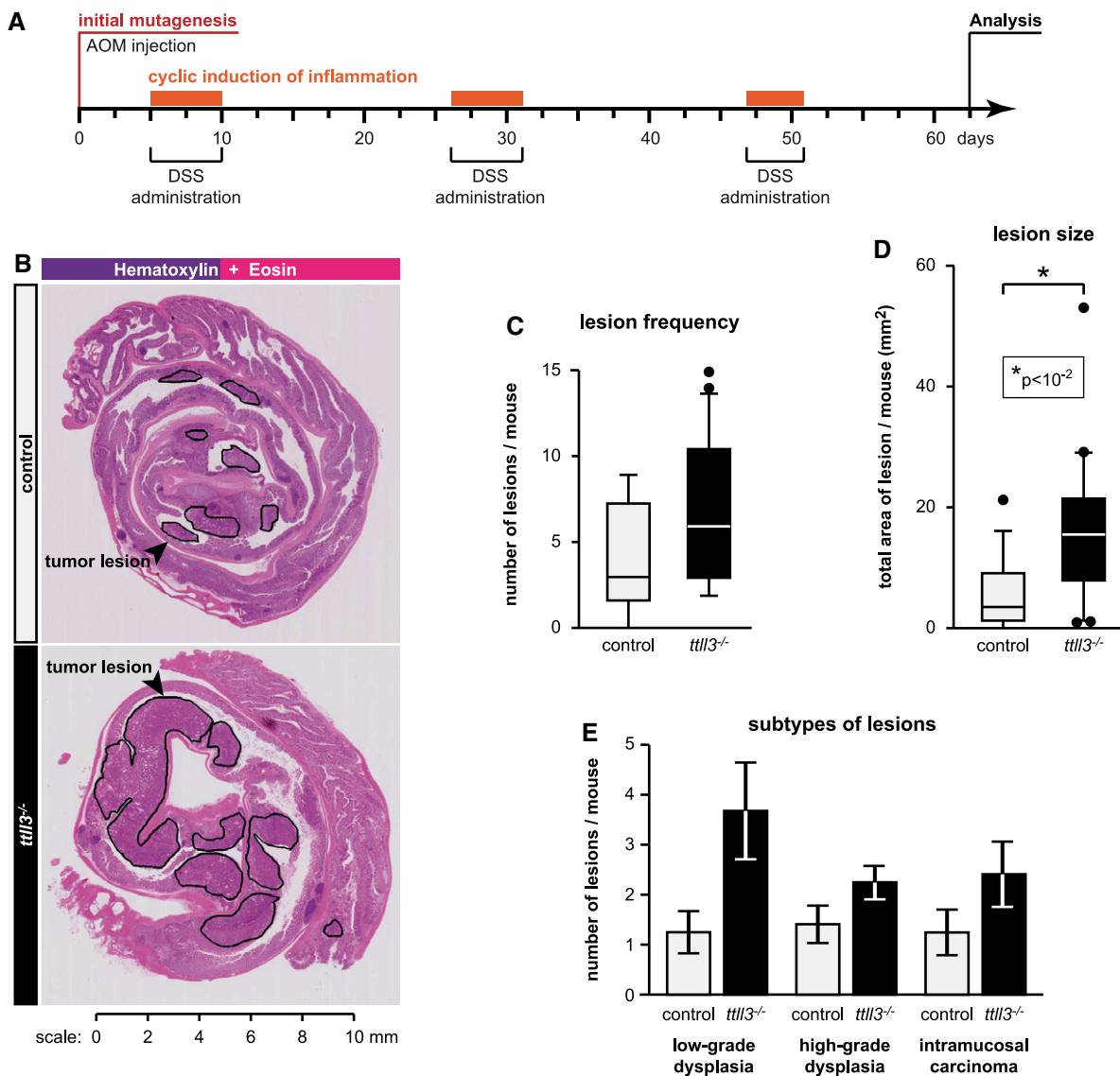
Figure 5. Loss of *TTLL3* promotes colon carcinogenesis.

Ten-week-old mice of the control ($n = 21$) and the *ttll3*$^{-/-}$ ($n = 23$) group were submitted to chemically induced colon carcinogenesis.

A   Experimental timeline for AOM/DSS-induced CRC.

B   Representative images of hematoxylin and eosin staining of paraffin-embedded colon sections prepared as "Swiss rolls". Single tumors are delimited by black lines.

C, D   Box plots of the average number of tumors per mouse (C) and the average total area of lesions per mouse (D) with a line indicating the median values. Dots represent values lower than 10% and > 90% of the mean values. Error bars are SD. *$P < 10^{-2}$.

E   Distributions of lesions from different subtypes (Supplementary Fig S4) between control ($n = 12$) and *ttll3*$^{-/-}$ ($n = 12$). Data are mean values between individual mice ± SEM.

The glycylase TTLL3 is downregulated in colorectal cancer

Similar to its murine ortholog, human *TTLL3* is an active glycylase expressed in most normal tissues (Supplementary Fig S5). The gene has previously been linked to human colon cancer by the identification of two cancer patients with two distinct somatic mutations in the *TTLL3* gene (Sjöblom *et al*, 2006). Both mutations lead to a loss of detectable enzymatic activity of TTLL3, suggesting that the enzyme could be directly involved in the development of colorectal cancer (Rogowski *et al*, 2009). To investigate whether loss-of-function mutations are frequent events in colorectal cancer (CRC),

we sequenced 30 cDNAs and 42 genomic DNAs within the enzymatically important conserved TTL domain of *TTLL3*. Since no additional mutations have been found in the tested samples, we concluded that the above described glycylase-inactivating mutations represent rare events in CRC. This is in agreement with a recent report showing that *TTLL3* is mutated in only one tumor among 276 CRCs using exome sequence analyses (Cancer Genome Atlas Network, 2012).

Next, we analyzed *TTLL3* expression levels in a large set of histopathologically well-characterized tumor samples from patients that had not received prior treatment. The samples were classified into

normal colon tissue, colorectal adenomas, primary colorectal carcinomas and matched liver metastases (Fig 6A). qRT-PCR analysis showed a significant downregulation of *TTLL3* expression in primary colorectal carcinomas and matched metastases, while

expression levels in the benign colorectal adenomas were similar to those of matched normal colon tissues (Fig 6B). These data unambiguously demonstrated that *TTLL3* is associated to CRC progression via the downregulation of its expression in colon carcinomas.
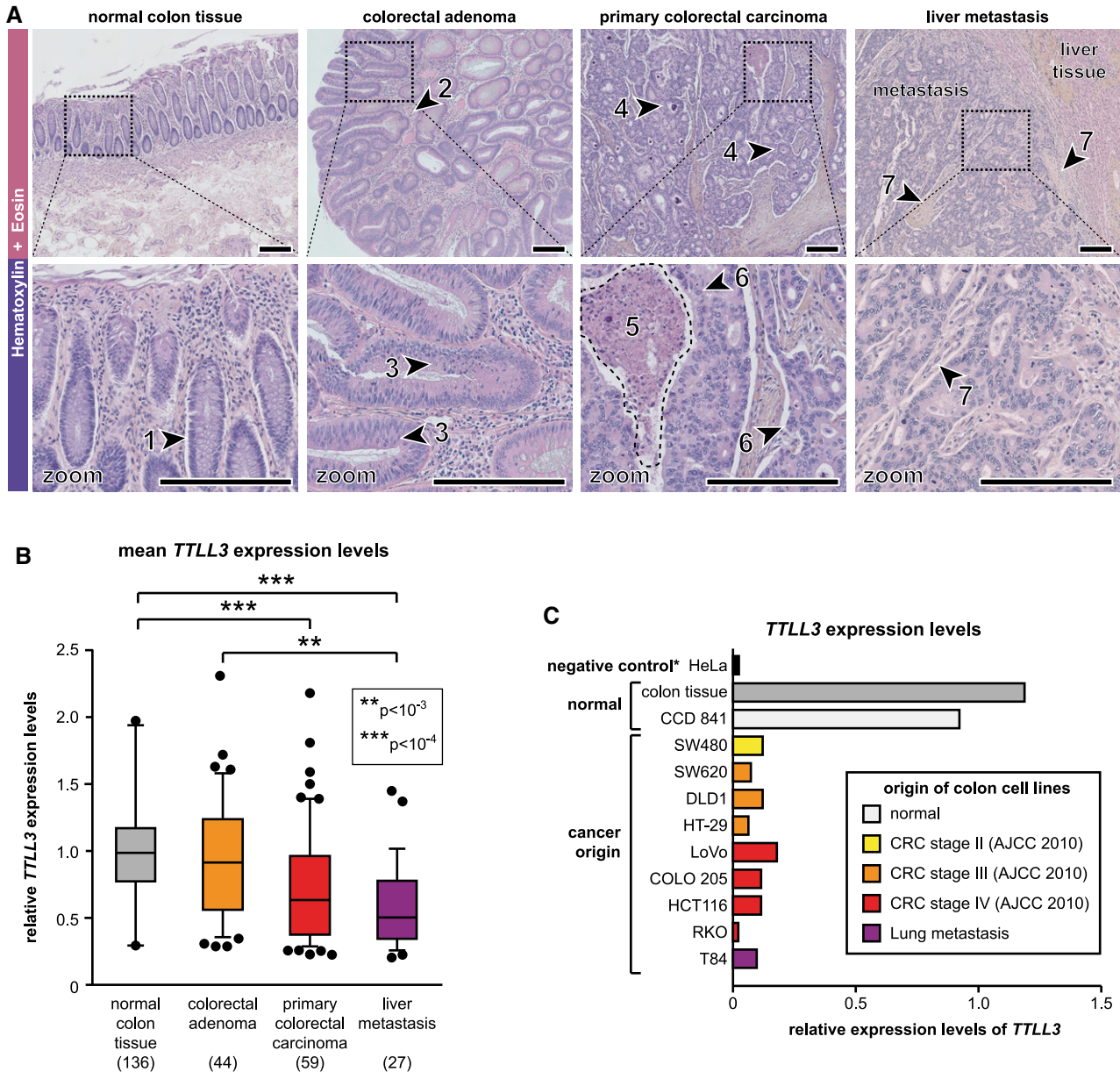
Figure 6.   Decreased *TTLL3* expression is linked to loss of primary cilia and colon carcinoma.

A   Histopathological characterization of tissues used for expression analysis shown in (B). Normal colon tissue shows polarized epithelial cells with small, round, basally located nuclei (1). Adenomas show maintenance of the integrity of the basement membrane (2), as well as alterations in epithelial polarity and cellular crowding (3). Colorectal carcinomas show architectural disorganization (e.g. cribriform growth pattern; 4) and necrosis of the tissue (5), as well as high nuclear pleomorphism (anisokaryosis and loss of nuclear polarity; 6). Liver metastases show marked desmoplastic stromal response (7) surrounding the invasive malignant glands. Scale bar is 200 μm.

B   qRT-PCR analysis of *TTLL3* expression in colon and tumor tissue samples from patients. Untreated human samples from colorectal adenomas (n = 44), primary colorectal carcinomas (n = 59), liver metastasis (n = 27) and matched normal adjacent colorectal tissues (n = 136) are compared. Expression levels are normalized to *TATA binding protein* (*TBP*) gene, and represented as mean values $\pm$ SD. Dots represent values lower than 1% (normal tissue) or 10% (other series) and > 99% (normal tissue) or 90% (other series) of the mean values. Significance values were determined with ANOVA (**$P < 10^{-3}$; ***$P < 10^{-4}$).

C   Expression levels of *TTLL3* in human colon cancer cell lines (for details see Supplementary Table S1) and the colonic epithelial cell line CCD841 by qRT-PCR. Normal colon tissue and HeLa cells are used as controls (*HeLa is a tumor cell line unable to grow cilia).

To investigate whether the downregulation of *TTLL3* expression is a general feature of human CRC, we analyzed seven established CRC-derived cell lines of different origin, as well as the colonic epithelial cell line CCD 841 with qRT-PCR. While *TTLL3* was expressed at similar levels in normal colon tissue and CCD 841, it was strongly downregulated in all tested CRC cell lines, which are characterized by different mutation profiles (Fig 6C; Supplementary Table S1). Thus, downregulation of *TTLL3* expression is a general feature of CRC that appears not to be associated with a specific tumor subtype.

Discussion

Posttranslational modifications of tubulin are thought to fine-tune MT functions in specific cells and tissues. Modifications that take place on the C-terminal tails of tubulin are involved in the regulation of interactions between MTs and associated proteins (reviewed in: Janke & Bulinski, 2011). The three principal modifications found in these tail domains are detyrosination, (poly)glutamylation and (poly)glycylation. While first insights into the molecular mechanisms that are controlled by detyrosination (Peris *et al*, 2006, 2009; Bieling *et al*, 2008) and polyglutamylation (Kubo *et al*, 2010; Lacroix *et al*, 2010) have been obtained, little is known about the roles and mechanisms of glycylation.

In contrast to other tubulin modifications, glycylation has so far only been detected in motile cilia and flagella in different organisms (Bré *et al*, 1996). In line with this rather restricted occurrence of glycylation, only three modifying enzymes are expressed in mammals (Rogowski *et al*, 2009), in contrast to nine glutamylating enzymes (van Dijk *et al*, 2007). Even more remarkably, only two of the mammalian glycylases, TTLL3 and TTLL8, are able to initiate glycylation on tubulin, while the third, elongating TTLL10 enzyme elongates pre-formed glycine side chains on tubulin. Considering that TTLL10 is enzymatically inactive in human (Rogowski *et al*, 2009) and that polyglycine side chains are generated very late in the development of motile ependymal cilia in mouse, it is assumed that the poly-character of glycylation is not essential in mammals. However, monoglycylation, generated by the initiating glycylases TTLL3 and TTLL8, is of key importance in the maintenance of motile cilia (Bosch Grau *et al*, 2013).

Almost nothing was so far known about the role of glycylation in primary cilia. Using MEFs and CECs, we now demonstrate that similar to motile cilia, primary cilia also depend on glycylation. However, while motile cilia disassembled completely in the absence of TTLL3 and TTLL8 (Bosch Grau *et al*, 2013), primary cilia are only reduced in numbers. The latter was observed in two entirely different cell types (CECs and MEFs) and thus puts forward a concept that partial loss of primary cilia in the absence of glycylation is a general feature, and not cell-type specific. While glycylation is important for primary cilia, it appears to be only one of several factors necessary to assemble and maintain the structures of these organelles on cells. Many cell lines that are commonly used in research have lost their ability to grow primary cilia, and often these cells do not express *TTLL3* or *TTLL8*. Re-expression of these genes, however, does not induce ciliogenesis in these cell lines (our unpublished observations).
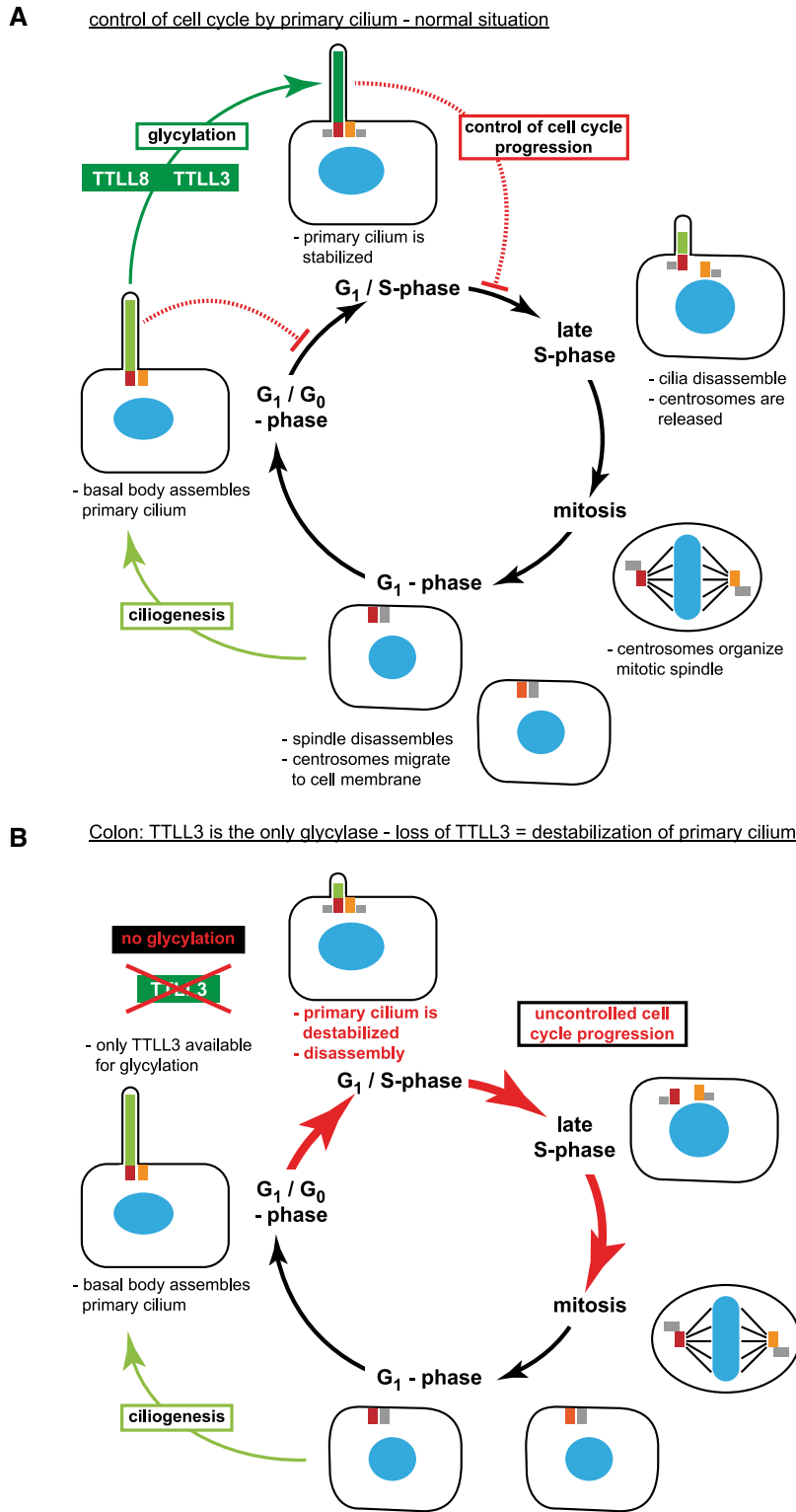
The fact that a knockout mouse for *TTLL3* showed no typical cilia-related phenotypes (Fliegauf *et al*, 2007) suggested that TTLL8

can functionally compensate loss of TTLL3 *in vivo*. However, this is not true for colon, a tissue with no expression of *TTLL8*. This tissue has so far been considered to have no primary cilia, which is most likely related to the difficulty to detect them. We partially overcame this problem using Arl13b, a primary cilia-specific marker, which allowed us to detect primary cilia in some but not all cells present in colon tissue sections. Despite this difficulty, we demonstrated a statistically significant reduction of the number of cilia in the colons of *ttll3*$^{-/-}$ mice as compared to controls, which is coherent with the strongly reduced number of primary cilia found on isolated *ttll3*$^{-/-}$ colon epithelial cells (CECs).

Primary cilia can execute different functions by regulating cell–cell communication and signaling (Gerdes *et al*, 2009; Goetz & Anderson, 2010), and notably cell division (Pugacheva *et al*, 2007; Kim *et al*, 2011; Li *et al*, 2011) and tissue homeostasis (Lin *et al*, 2003; Croyle *et al*, 2011; Saqui-Salces *et al*, 2012; Wilson *et al*, 2012). The colon epithelium is a tissue with a particularly high proliferation rate and cell turnover. Cells are generated from stem cells located at the base of the colon crypts and then migrate within 5 days toward the top of the crypts, where they are removed by mechanical shedding, which is associated with an anoikis-type of cell death (Medema & Vermeulen, 2011). Despite this high proliferation rate, cell division is strictly controlled, as dividing cells are only observed in the bottom of the crypts. It was thus remarkable to observe that the number of dividing cells is more than doubled in *ttll3*$^{-/-}$ mice, and dividing cells are found in regions of the crypts where no proliferation is seen in controls. Thus, we conclude that absence of TTLL3 might perturb cell proliferation (Fig 7), though the pathways affected by the loss of glycylation remain to be identified, and potential effects of glycylation on other proteins is yet unknown. Strikingly, this overproliferation had no visible effect on the global architecture of this organ, even in aged mice. This suggests that the high turnover of the colon epithelium can tolerate increased cell proliferation and assure tissue homeostasis by further accelerating turnover. The defect only becomes apparent upon induction of tumorigenesis, when the higher proliferation rates of the colonic epithelial cells appear to promote a more rapid tumor development.

Our findings suggest that perturbations of primary cilia can promote cancer development in colon if other cancer-promoting events occur. Indeed, the study that had discovered the first CRC-related mutations in *TTLL3* also identified another ciliary gene related to CRC, *polycystic kidney and hepatic disease 1* (*PKHD1*; Sjöblom *et al*, 2006). While absence of the glycylase TTLL3 has a selective effect on colon tissue (which does, in contrast to other tissues, not express TTLL8), other factors that perturb glycylation and thus affect the assembly or maintenance of primary cilia might similarly amplify cancer development in other tissues (Fig 7).

In conclusion, we have demonstrated a role of posttranslational glycylation for primary cilia, suggesting that this particular post-translational modification is involved in the stabilization of ciliary axonemes. Loss of primary cilia in colon epithelium led to aberrations in cell proliferation, but not to apparent perturbations of tissue homeostasis. In contrast, the ciliary defects had a significant impact on cancer development. Analysis of tumors from patients with CRC confirmed that lower expression levels of *TTLL3* provide a risk factor for colon carcinoma development, suggesting that *TTLL3* has the potential to become a prognostic marker for CRC.

A   control of cell cycle by primary cilium - normal situation

B   Colon: TTLL3 is the only glycylase - loss of TTLL3 = destabilization of primary cilium

Figure 7.   A model for the potential role of TTLL3 in the cell cycle.
Schematic representations of the different phases of the cell cycle with cells growing primary cilia in G_1 or G_0 phase. Our results indicate that these cilia are stabilized by glycylation that can be catalyzed by either TTLL3, or by TTLL8 or by both enzymes (A). In the colon, only TTLL3 can carry out this role, and in the case of mutation, downregulation or loss of TTLL3, glycylation is disrupted (B). As a result, cilia are destabilized and lost in a non-controlled manner. Considering the role of primary cilia in cell cycle regulation (Pugacheva *et al*, 2007), we propose a model in which the ciliary disassembly directly determines the advancement of the cell cycle during S phase and at the transition to mitosis (A). Absence of cilia would thus lead to uncontrolled entry and passage of the cell cycle (B). Schematic representation inspired by Ishikawa and Marshall (Ishikawa & Marshall, 2011).

Materials and Methods

Patient samples

Untreated human samples from colorectal adenomas, adenocarcinoma, liver metastasis and matched normal adjacent colorectal tissues were collected by the surgical oncology and stored in the Biological Resource Center (BRC) of the Institut Curie, France (permission No. A10-024). According to French regulations, patients were informed of research performed with the biological specimens obtained during their treatment and did not express opposition. Disease stage of CRC was based on 7th revised edition of the AJCC Colorectal Cancer.

Animal experimentation

Mouse experiments were performed in strict accordance with the guidelines of the European Community (86/609/EEC) and the French National Committee (87/848) for care and use of laboratory animals. We used the B6N-ttll3[tm1a(EUCOMM)Wtsi] mice carrying *LacZ* reporter cassette that is inserted into the *TTLL3* gene region. Expression of the *LacZ* gene is driven by the *TTLL3* gene promoter and allows localization of *TTLL3* expression in tissues (Fig 2B), while at the same time, the expression of the *TTLL3* gene is disrupted (Fig 2C).

Histology and immunohistochemistry

Organs were fixed in formalin solution for 16 h. Histological examination was performed on paraffin-embedded sections and stained for histopathological analysis. Immunohistochemistry was performed on formalin-fixed and paraffin-embedded tissues cut into 4-μm sections. After blocking with 10% goat serum, samples were incubated with primary antibody for 2 h. Secondary antibodies were either HRP-coupled anti-mouse or anti-rabbit IgGs, visualized with 3,3′-diaminobenzidine (DAB), or fluorescent-labeled anti-mouse/rabbit antibodies. DNA was stained with 20 μg/ml 4′,6-diamidino-2-phenylindole (DAPI).

AOM/DSS model, tumor histology and histological grading of tumors

For colitis-associated carcinogenesis, mice were intraperitoneally injected with azoxymethane (AOM), followed by three cycles of 2.5% (w/v) dextrane sodium sulfate (DSS) administered in the drinking water (Fig 5A). Colons were histologically analyzed as described above.

Histological grading of AOM/DSS-induced tumors was determined with blinded genotype according to Vienna classification of gastrointestinal epithelial neoplasia (Schlemper *et al*, 2000).

BrdU incorporation proliferation assay

Twelve-week-old mice were intraperitoneally injected with 100 μg/g bromodeoxyuridine (BrdU). Colons were dissected 2 h or 5 days following injection. Proliferating cells were detected with anti-BrdU antibody, and BrdU-positive cells were quantified from at least three animals per condition.

β-galactosidase staining

To visualize *TTLL3* promoter-driven lacZ expression, histological sections were stained with 5-bromo-4-chloro-3-indolyl-beta-D-galactopyranoside (X-gal).

Cell culture

Cells were grown at 37°C, 5% CO_2 and 100% humidity. Cell lines were cultured in DMEM medium containing 10% fetal bovine serum.

Mouse embryonic fibroblasts (MEF)

Cells were isolated from mouse embryos at embryonic day 13.5 (E13.5). Tissues apart from heads and internal organs were digested with 0.05% trypsin, and cells were dissociated and grown in DMEM medium/10% FBS, 55 μM β-mercaptoethanol and 100 μM of nonessential amino acids. MEFs were transfected with JetPEI. For ciliogenesis, MEFs were cultured on coverslips until reaching confluence and subsequently serum-starved for 24 h. Forty-eight hours after transfection, cells were fixed with −20°C methanol and submitted to immunofluorescence.

Primary colon epithelial cells (CEC)

CECs were isolated from mice at postnatal day 4 (P4). Colons were trypsinized, and cells were dissociated, filtered and grown in DMEM-F12 (1:1) medium with 20% FBS on fibronectin-coated coverslips. Upon confluence, cells were serum-starved for 24 or 48 h for ciliogenesis, fixed with −20°C methanol and submitted to immunofluorescence.

For cell cycle analysis, CECs were cultured in plastic dishes and fixed after 48 h with -20°C 70% ethanol for 2 h. DNA was stained with 7-aminoactinomycin D (7-AAD) in the presence of 0.1% Triton X-100 and 100 μg/ml RNase at 37°C for 1 h. The DNA content per cell was measured by flow cytometry on a FACSCalibur.

Microscopy and imaging

Histological slides were scanned using Nanozoomer 2.0 HT scanner with a 40× objective and visualized with the ndpi viewer. Fluorescent images were acquired on a brightfield microscope (Leica) using Metamorph software or inverted Confocal SP5 (Leica) using the Leica LAS AF software. Images were processed with ImageJ. Fluorescent secondary antibodies were labeled with Alexa 488, 568 and 647 fluorophores. Raw images were assembled and adjusted with Adobe Photoshop.

RT-PCR and qRT-PCR

RNA was extracted from homogenized mouse organs or from cells using TRIzol reagent following the standard protocol. RNA was translated to cDNA with first-strand cDNA synthesis kit using the dT_{18} primer. PCRs were carried out using standard protocols.

Quantitative RT-PCR was applied under standard conditions using the SYBR Green Master Mix kit on the ABI Prism 7900 Sequence Detection System. The relative mRNA expression levels of

each gene were expressed as the N-fold difference in target gene expression relative to the *TBP* gene.

Statistical analysis

Acknowledgements

Author contributions

CR designed and performed most of the experiments, analyzed data and wrote the manuscript; LP, VL, OT, TG, SV, and BL performed experiments and analyzed data; PMS and PM performed experiments; DM analyzed data; WC, JPM, and IB designed experiments, analyzed data, and had critical input into the manuscript preparation; MH and CJ conceived, designed and performed experiments, analyzed data, and wrote the manuscript.

Conflict of interest

The authors declare that they have no conflict of interest.

References

Audebert S, Koulakoff A, Berwald-Netter Y, Gros F, Denoulet P, Eddé B (1994) Developmental regulation of polyglutamylated alpha- and beta-tubulin in mouse brain neurons. *J Cell Sci* 107: 2313−2322

Bieling P, Kandels-Lewis S, Telley IA, van Dijk J, Janke C, Surrey T (2008) CLIP-170 tracks growing microtubule ends by dynamically recognizing composite EB1/tubulin-binding sites. *J Cell Biol* 183: 1223−1233

Bobinnec Y, Moudjou M, Fouquet JP, Desbruyeres E, Eddé B, Bornens M (1998) Glutamylation of centriole and cytoplasmic tubulin in proliferating non-neuronal cells. *Cell Motil Cytoskeleton* 39: 223−232

Bosch Grau M, Gonzalez Curto G, Rocha C, Magiera MM, Marques Sousa P, Giordano T, Spassky N, Janke C (2013) Tubulin glycylases and glutamylases have distinct functions in stabilization and motility of ependymal cilia. *J Cell Biol* 202: 441−451

Bré MH, Redeker V, Quibell M, Darmanaden-Delorme J, Bressac C, Cosson J, Huitorel P, Schmitter JM, Rossier J, Johnson T, Adoutte A, Levilliers N (1996) Axonemal tubulin polyglycylation probed with two monoclonal antibodies: widespread evolutionary distribution, appearance during spermatozoan maturation and possible function in motility. *J Cell Sci* 109: 727−738

Bré MH, Redeker V, Vinh J, Rossier J, Levilliers N (1998) Tubulin polyglycylation: differential posttranslational modification of dynamic cytoplasmic and stable axonemal microtubules in Paramecium. *Mol Biol Cell* 9: 2655−2665

Cancer Genome Atlas Network (2012) Comprehensive molecular characterization of human colon and rectal cancer. *Nature* 487: 330−337

Caspary T, Larkins CE, Anderson KV (2007) The graded response to Sonic Hedgehog depends on cilia architecture. *Dev Cell* 12: 767−778

Cevik S, Hori Y, Kaplan OI, Kida K, Toivenon T, Foley-Fisher C, Cottell D, Katada T, Kontani K, Blacque OE (2010) Joubert syndrome Arl13b functions at ciliary membranes and stabilizes protein transport in *Caenorhabditis elegans*. *J Cell Biol* 188: 953−969

Croyle MJ, Lehman JM, O'Connor AK, Wong SY, Malarkey EB, Iribarne D, Dowdle WE, Schoeb TR, Verney ZM, Athar M, Michaud EJ, Reiter JF, Yoder BK (2011) Role of epidermal primary cilia in the homeostasis of skin and hair follicles. *Development* 138: 1675−1685

van Dijk J, Rogowski K, Miro J, Lacroix B, Eddé B, Janke C (2007) A targeted multienzyme mechanism for selective microtubule polyglutamylation. *Mol Cell* 26: 437−448

Eddé B, Rossier J, Le Caer JP, Desbruyeres E, Gros F, Denoulet P (1990) Posttranslational glutamylation of alpha-tubulin. *Science* 247: 83−85

Fliegauf M, Benzing T, Omran H (2007) When cilia go bad: cilia defects and ciliopathies. *Nat Rev Mol Cell Biol* 8: 880−893

Gagnon C, White D, Cosson J, Huitorel P, Eddé B, Desbruyeres E, Paturle-Lafanechere L, Multigner L, Job D, Cibert C (1996) The polyglutamylated lateral chain of alpha-tubulin plays a key role in flagellar motility. *J Cell Sci* 109: 1545−1553

Gerdes JM, Davis EE, Katsanis N (2009) The vertebrate primary cilium in development, homeostasis, and disease. *Cell* 137: 32−45

Goetz SC, Anderson KV (2010) The primary cilium: a signalling centre during vertebrate development. *Nat Rev Genet* 11: 331−344

Ishikawa H, Marshall WF (2011) Ciliogenesis: building the cell's antenna. *Nat Rev Mol Cell Biol* 12: 222−234

Janke C, Bulinski JC (2011) Post-translational regulation of the microtubule cytoskeleton: mechanisms and functions. *Nat Rev Mol Cell Biol* 12: 773−786

Kim S, Zaghloul NA, Bubenshchikova E, Oh EC, Rankin S, Katsanis N, Obara T, Tsiokas L (2011) Nde1-mediated inhibition of ciliogenesis affects cell cycle re-entry. *Nat Cell Biol* 13: 351−360

Kubo T, Yanagisawa H-a, Yagi T, Hirono M, Kamiya R (2010) Tubulin polyglutamylation regulates axonemal motility by modulating activities of inner-arm dyneins. *Curr Biol* 20: 441−445

Lacroix B, van Dijk J, Gold ND, Guizetti J, Aldrian-Herrada G, Rogowski K, Gerlich DW, Janke C (2010) Tubulin polyglutamylation stimulates spastin-mediated microtubule severing. *J Cell Biol* 189: 945–954

Lascano V, Fernandez Zabalegui L, Cameron K, Guadagnoli MM, Jansen M, Burggraaf M, Versloot M, Rodermond H, van der Loos CM, Carvalho-Pinto C, Kalthoff H, Medema JP, Hahne M (2012) The TNF family member APRIL promotes colorectal tumorigenesis. *Cell Death Differ* 19: 1826–1835

Lee JE, Silhavy JL, Zaki MS, Schroth J, Bielas SL, Marsh SE, Olvera J, Brancati F, Iannicelli M, Ikegami K, Schlossman AM, Merriman B, Attie-Bitach T, Logan CV, Glass IA, Cluckey A, Louie CM, Lee JH, Raynes HR, Rapin I *et al* (2012) CEP41 is mutated in Joubert syndrome and is required for tubulin glutamylation at the cilium. *Nat Genet* 44: 193–199

Lee G-S, He Y, Dougherty EJ, Jimenez-Movilla M, Avella M, Grullon S, Sharlin DS, Guo C, Blackford JA, Awasthi S, Zhang Z, Armstrong SP, London EC, Chen W, Dean J, Simons SS (2013) Disruption of Ttll5/Stamp gene (Tubulin tyrosine ligase-like protein 5/SRC-1 and TIF2 associated modulatory protein gene) in male mice causes sperm malformation and infertility. *J Biol Chem* 21: 15167–15180

Li A, Saito M, Chuang J-Z, Tseng Y-Y, Dedesma C, Tomizawa K, Kaitsuka T, Sung C-H (2011) Ciliary transition zone activation of phosphorylated Tctex-1 controls ciliary resorption, S-phase entry and fate of neural progenitors. *Nat Cell Biol* 13: 402–411

Lin F, Hiesberger T, Cordes K, Sinclair AM, Goldstein LSB, Somlo S, Igarashi P (2003) Kidney-specific inactivation of the KIF3A subunit of kinesin-II inhibits renal ciliogenesis and produces polycystic kidney disease. *Proc Natl Acad Sci USA* 100: 5286–5291

Medema JP, Vermeulen L (2011) Microenvironmental regulation of stem cells in intestinal homeostasis and cancer. *Nature* 474: 318–326

Million K, Larcher J, Laoukili J, Bourguignon D, Marano F, Tournier F (1999) Polyglutamylation and polyglycylation of alpha- and beta-tubulins during *in vitro* ciliated cell differentiation of human respiratory epithelial cells. *J Cell Sci* 112: 4357–4366

Pathak N, Obara T, Mangos S, Liu Y, Drummond IA (2007) The zebrafish fleer gene encodes an essential regulator of cilia tubulin polyglutamylation. *Mol Biol Cell* 18: 4353–4364

Pathak N, Austin CA, Drummond IA (2011) Tubulin tyrosine ligase-like genes ttll3 and ttll6 maintain Zebrafish cilia structure and motility. *J Biol Chem* 286: 11685–11695

Peris L, Thery M, Faure J, Saoudi Y, Lafanechere L, Chilton JK, Gordon-Weeks P, Galjart N, Bornens M, Wordeman L, Wehland J, Andrieux A, Job D (2006) Tubulin tyrosination is a major factor affecting the recruitment of CAP-Gly proteins at microtubule plus ends. *J Cell Biol* 174: 839–849

Peris L, Wagenbach M, Lafanechere L, Brocard J, Moore AT, Kozielski F, Job D, Wordeman L, Andrieux A (2009) Motor-dependent microtubule disassembly driven by tubulin tyrosination. *J Cell Biol* 185: 1159–1166

Pugacheva EN, Jablonski SA, Hartman TR, Henske EP, Golemis EA (2007) HEF1-dependent Aurora A activation induces disassembly of the primary cilium. *Cell* 129: 1351–1363

Redeker V, Levilliers N, Schmitter JM, Le Caer JP, Rossier J, Adoutte A, Bré MH (1994) Polyglycylation of tubulin: a posttranslational modification in axonemal microtubules. *Science* 266: 1688–1691

Rogowski K, Juge F, van Dijk J, Wloga D, Strub J-M, Levilliers N, Thomas D, Bré MH, Van Dorsselaer A, Gaertig J, Janke C (2009) Evolutionary divergence of enzymatic mechanisms for posttranslational polyglycylation. *Cell* 137: 1076–1087

Saqui-Salces M, Dowdle WE, Reiter JF, Merchant JL (2012) A high-fat diet regulates gastrin and acid secretion through primary cilia. *FASEB J* 26: 3127–3139

Schlemper RJ, Riddell RH, Kato Y, Borchard F, Cooper HS, Dawsey SM, Dixon MF, Fenoglio-Preiser CM, Flejou JF, Geboes K, Hattori T, Hirota T, Itabashi M, Iwafuchi M, Iwashita A, Kim YI, Kirchner T, Klimpfinger M, Koike M, Lauwers GY *et al* (2000) The Vienna classification of gastrointestinal epithelial neoplasia. *Gut* 47: 251–255

Scholzen T, Gerdes J (2000) The Ki-67 protein: from the known and the unknown. *J Cell Physiol* 182: 311–322

Sjöblom T, Jones S, Wood LD, Parsons DW, Lin J, Barber TD, Mandelker D, Leary RJ, Ptak J, Silliman N, Szabo S, Buckhaults P, Farrell C, Meeh P, Markowitz SD, Willis J, Dawson D, Willson JKV, Gazdar AF, Hartigan J *et al* (2006) The consensus coding sequences of human breast and colorectal cancers. *Science* 314: 268–274

Suryavanshi S, Edde B, Fox LA, Guerrero S, Hard R, Hennessey T, Kabi A, Malison D, Pennock D, Sale WS, Wloga D, Gaertig J (2010) Tubulin glutamylation regulates ciliary motility by altering inner dynein arm activity. *Curr Biol* 20: 435–440

Suzuki R, Kohno H, Sugie S, Tanaka T (2004) Sequential observations on the occurrence of preneoplastic and neoplastic lesions in mouse colon treated with azoxymethane and dextran sodium sulfate. *Cancer Sci* 95: 721–727

Tanaka T, Kohno H, Suzuki R, Yamada Y, Sugie S, Mori H (2003) A novel inflammation-related mouse colon carcinogenesis model induced by azoxymethane and dextran sodium sulfate. *Cancer Sci* 94: 965–973

Tetsu O, McCormick F (1999) Beta-catenin regulates expression of cyclin D1 in colon carcinoma cells. *Nature* 398: 422–426

Wilson SL, Wilson JP, Wang C, Wang B, McConnell SK (2012) Primary cilia and Gli3 activity regulate cerebral cortical size. *Dev Neurobiol* 72: 1196–1212

Wloga D, Webster DM, Rogowski K, Bré MH, Levilliers N, Jerka-Dziadosz M, Janke C, Dougan ST, Gaertig J (2009) TTLL3 Is a tubulin glycine ligase that regulates the assembly of cilia. *Dev Cell* 16: 867–876

Xia L, Hai B, Gao Y, Burnette D, Thazhath R, Duan J, Bré MH, Levilliers N, Gorovsky MA, Gaertig J (2000) Polyglycylation of tubulin is essential and affects cell motility and division in *Tetrahymena thermophila*. *J Cell Biol* 149: 1097–1106